

Detoxification of Domoic Acid from *Pseudo-nitzschia* by Gut Microbiota in *Acartia erythraea*

Qihang Li¹, Jiawei Chen¹, Zhimeng Xu¹, Lixia Deng¹, Xihe Fang¹, Shuwen Zhang², Xiaodong Zhang¹, Huo Xu¹, Shen Lin¹, and Hongbin Liu¹

¹Hong Kong University of Science and Technology

²South China Normal University

February 07, 2025

Abstract

Domoic acid (DA) is a neurotoxin produced by certain species of *Pseudo-nitzschia* (*PSN*) that can cause damage to neural tissues and can be fatal to marine animals. Copepods, direct consumers of *PSN*, exhibit remarkable resistance to DA. Given that gut microbiota facilitate various detoxification processes in copepods, we hypothesize that gut microbiota may play a crucial role in aiding copepods in DA detoxification. In this study, we investigated the detoxification capability of copepod gut microbiota by feeding both wild-type and gut-microbiota-free *Acartia erythraea* toxic *PSN*. Our results demonstrated that, although DA suppressed the growth of *A. erythraea*, the presence of gut microbiota enhanced the survival of copepods exposed to a DA diet. We subsequently feed *A. erythraea* both toxic and non-toxic *PSN*, and explored the potential mechanisms of DA detoxification through amplicon and metatranscriptome approaches. We identified both anaerobic and aerobic DA detoxification pathways in copepod gut bacteria, mediated by the genera *Aureispira*, *Tenacibaculum*, *Pseudoalteromonas*, *Shewanella*, and *Vibrio*. In the anaerobic pathway, DA could be biotransformed into detoxification products through a series of main degradation steps, including decarboxylation, dehydrogenation, carboxylation, and multiple β -oxidation processes. In the aerobic pathway, DA undergoes reactions including hydration, dehydrogenation, hydrolysis, hydroxylation, and oxidation, resulting in the formation of terminal detoxification products. Overall, our findings elucidate the mechanisms by which copepod gut microbiota detoxify DA, thereby advancing our understanding of copepod resilience in the face of a toxic diet.

Detoxification of Domoic Acid from *Pseudo-nitzschia* by Gut Microbiota in *Acartia erythraea*

Qihang Li¹, Jiawei Chen^{1*}, Zhimeng Xu¹, Lixia Deng¹, Xihe Fang¹, Shuwen Zhang², Xiaodong Zhang¹, Huo Xu¹, Shen Lin¹, Hongbin Liu^{1,3*}

¹Department of Ocean Science, the Hong Kong University of Science and Technology, Hong Kong SAR, China

²Guangzhou Provincial Key Laboratory of Biotechnology for Plant Development, Guangzhou Key Laboratory of Subtropical Biodiversity and Biomonitoring, School of Life Science, South China Normal University, Guangzhou, China

³State Key Laboratory of Marine Pollution, Hong Kong, China

*Corresponding authors:

Hongbin Liu

Email: liuhb@ust.hk

Jiawei Chen

Email: jchenek@connect.ust.hk

Abstract

Domoic acid (DA) is a neurotoxin produced by certain species of *Pseudo-nitzschia* (*PSN*) that can cause damage to neural tissues and can be fatal to marine animals. Copepods, direct consumers of *PSN*, exhibit remarkable resistance to DA. Given that gut microbiota facilitate various detoxification processes in copepods, we hypothesize that gut microbiota may play a crucial role in aiding copepods in DA detoxification. In this study, we investigated the detoxification capability of copepod gut microbiota by feeding both wild-type and gut-microbiota-free *Acartia erythraea* toxic *PSN*. Our results demonstrated that, although DA suppressed the growth of *A. erythraea*, the presence of gut microbiota enhanced the survival of copepods exposed to a DA diet. We subsequently feed *A. erythraea* both toxic and non-toxic *PSN*, and explored the potential mechanisms of DA detoxification through amplicon and metatranscriptome approaches. We identified both anaerobic and aerobic DA detoxification pathways in copepod gut bacteria, mediated by the genera *Aureispira*, *Tenacibaculum*, *Pseudoalteromonas*, *Shewanella*, and *Vibrio*. In the anaerobic pathway, DA could be biotransformed into detoxification products through a series of main degradation steps, including decarboxylation, dehydrogenation, carboxylation, and multiple β -oxidation processes. In the aerobic pathway, DA undergoes reactions including hydration, dehydrogenation, hydrolysis, hydroxylation, and oxidation, resulting in the formation of terminal detoxification products. Overall, our findings elucidate the mechanisms by which copepod gut microbiota detoxify DA, thereby advancing our understanding of copepod resilience in the face of a toxic diet.

Keywords: *Pseudo-nitzschia*, Domoic acid, Gut microbiota, Detoxification, Copepods, Metatranscriptome

Introduction

The genus *Pseudo-nitzschia* (*PSN*) comprises a group of pennate, chain-forming diatoms that are prevalent in marine environments (Bates et al. 2018). In China's coastal waters, *PSN* frequently appears in phytoplankton communities (Chen et al. 2005; Lü et al. 2012), and can trigger harmful algal blooms. Notably, four such blooms occurred in Daya Bay between 1990 and 2005 (Chen et al. 2005; Liu et al. 2016). The Agriculture, Fisheries and Conservation Department (<http://www.afcd.gov.hk>) has documented over 20 *PSN* blooms in Hong Kong waters since 2009, with the largest bloom affecting an area of 150 km², leading to significant ecological and fishery damage. Some *PSN* species produce a neurotoxin known as domoic acid (DA), with 29 out of 63 species known to produce this toxin (Lundholm 2024; Niu et al. 2024). In China, 11 of 31 *PSN* species have been identified as DA producers (Li et al. 2017; Dong et al. 2020). Interestingly, several *PSN* species previously deemed non-toxic have been found to produce DA in Chinese coastal waters (Li et al. 2017; Huang et al. 2019; Dong et al. 2020). For instance, five species isolated from Victoria Harbour and Mirs Bay were newly reported to produce DA, with concentrations ranging from 0.012 to 40.3 fg cell⁻¹ (Dong et al. 2020). Bates et al. (2018) proposed that under suitable conditions, all *PSNs* could potentially produce DA.

DA can travel through the food web, affecting higher trophic levels such as seabirds, whales, and seals (Leandro et al. 2010; Tammilehto et al. 2012; D'Agostino et al. 2017). It also causes amnesic shellfish poisoning in humans (Wright et al. 1990). The presence of toxic DA has led to considerable marine animal mortality and economic losses in North American and European coastal waters (Bates et al. 2018). More countries are reporting issues related to this diatom genus (Bates, Garrison, and Horner 1998; Bates et al. 2018). Recent research indicates that DA can also hinder denitrification and Anammox processes, which are vital for nitrogen removal in sediments, thus affecting nitrogen cycling (Li et al. 2023).

While DA is linked to widespread poisoning in marine mammals and birds, copepods show some resistance to this toxin. Research suggests that copepod species like *Calanus sp.* and *Acartia sp.* consume toxic *PSNs* without significant deterrence and do not preferentially select non-toxic prey (Tester et al. 2000; Maneiro et al. 2005; Leandro et al. 2010; Harardóttir et al. 2019). Moreover, studies have shown no significant difference in mortality rates, egg production and hatching rates, between zooplankton consuming toxic and non-toxic *PSNs* (Lincoln et al. 2001; Miesner et al. 2016). However, other studies indicates that DA does affect

copepods. Although grazing rates may not decrease significantly, physiological stress is observed in copepods consuming DA-producing *Pseudo-nitzschia seriata*, as shown by gene expression profiles (Harardóttir et al. 2019). Additionally, Arctic copepods like *Calanus hyperboreus* and *C. glacialis* exhibit reduced escape responses after feeding on DA-producing diatoms (Harardóttir et al. 2018). Compared to higher trophic level organisms, copepods and other zooplankton accumulate relatively low levels of DA (Liefer et al. 2013), which might explain their reduced sensitivity to this toxin.

Some researchers suggest that the gut microbiota of zooplankton may help detoxify this toxin, reducing its harmful effects (Li et al. 2019; Gorokhova et al. 2021; Yang et al. 2024). The zooplankton gut provides a unique microhabitat for microorganisms, offering specific environmental conditions and sources of carbon and nutrients. Gut microbiota play a vital role by supplying essential nutrients and vitamins that enhance the host’s digestive capacity (Harris 1993). While bacteria can enter the gut through detritus or planktonic prey, studies show that copepod gut communities differ from those in the surrounding seawater, indicating specialized, long-term microbial communities (Shoemaker and Moisaner 2017). Recent findings reveal that variations in gut microbiota, influenced by environmental factors and host genotype, can mediate *Daphnia*’s tolerance to toxic cyanobacteria, highlighting the microbiota’s role in adapting to toxic diets (Macke et al. 2017). Moreover, zooplankton neonates from mothers zooplankton fed toxic algae showed improved growth and reproduction compared to those from mothers consuming non-toxic algae, suggesting a possible maternal transfer of beneficial gut microbiota (Lyu et al. 2016; Macke et al. 2017). Prior research in our laboratory has demonstrated that *Daphnia* gut microbiota can detoxify silver nanoparticles (AgNPs) by converting silver ions (Ag⁺) to less harmful forms and neutralizing them with flagellin protein (Li et al. 2019). Additionally, the maternal transfer of gut microbiota may enable younger generations to adapt to toxicity more swiftly (Li, Wang, and Liu 2022). Consequently, the gastrointestinal microorganisms of zooplankton are increasingly recognized as crucial factors influencing host physiological condition and fitness, especially regarding toxin exposure. However, there remains limited knowledge about the detoxification processes and molecular mechanisms of zooplankton gut microbiota.

In this study, we explored the effects of toxic (*P. cuspidata*) and non-toxic PSNs (*P. brasiliiana*) on *Acartia erythraea*, a dominant copepod species in Hong Kong coastal waters, using physiological assessments and multi-omics techniques. Our goal was to test the hypothesis that copepod gut microbiota aids in detoxifying DA. Specifically, we sought to identify which gut microbiota taxa in *A. erythraea* are involved in DA detoxification and to uncover molecular evidence of potential detoxification pathways.

Materials and methods

2.1 The culture of algae and copepods

Two species of PSNs, *P. cuspidata* (toxic) and *P. brasiliiana* (non-toxic), were isolated from the coastal waters of Guangdong, China, and used as prey for copepods. The algae were cultured in 1-liter flasks containing 0.2 µm-filtered sterilized seawater supplemented with f/2 medium (Guillard and Ryther 1962). Cultures were maintained in a temperature-controlled walk-in chamber at 22°C with a 14:10 hour light:dark cycle. To ensure the freshness of the algae and adequate levels of DA, the PSNs were used for experiments during the early stationary phase. Intracellular DA content was measured the day before the experiment using the method described by Niu et al. (2024).

Copepods (*A. erythraea*) were collected from Port Shelter, Hong Kong, using a WP2 net with a mesh size of 200 µm. The collected copepods were filtered through 1000 µm and 450 µm meshes to remove other species and immature individuals. We selected copepods that passed through the 1000 µm net but were retained by the 450 µm net. Individuals were identified under a dissection microscope (Olympus IX51), and the dominant species, *A. erythraea* were isolated. The selected copepods were cultured in multiple 50 L tanks filled with 0.2 µm-filtered seawater under a 12:12 hour light:dark cycle. Saturating amounts of PSNs were also provided to the selected copepods, and continuous aeration maintained oxygen levels and prevented PSNs from settling. Dead copepods were promptly removed, and the seawater was changed daily.

2.2 Antibiotic experiment and physiological monitoring of *A. erythraea* (Expt1.)

Copepods were categorized into five groups: the first two groups were fed *P. brasiliiana* and *P. cuspidata*, respectively; the second two groups received the same algal diets with the addition of antibiotics; and the final group served as a control with no supplements. The survival rate of copepods in each group was monitored over five days by culturing them in 2-liter beakers, with 50 individuals per beaker and three replicates per group. Additionally, ingestion and respiration rates were measured for the first two groups (Fig. 1).

Three commercially available antibiotics—ciprofloxacin, sulfamethoxazole, and trimethoprim—were used at low concentrations of 5 mg/L, as recommended by Edlund et al. (2012). These three antibiotics, which possess different antibacterial mechanisms, were combined to maximize the elimination of gut microbiota. To evaluate the effectiveness of the antibiotic treatment, we employed a BD FACSCelesta flow cytometer to measure the absolute abundance of copepod gut microbiota before and after antibiotic application (24 hours post treatment). Copepod guts were dissected and homogenized using a 40 μm cell strainer (#93040; SPL Life Sciences). The filtrates were carefully collected, diluted to a final volume of 10 mL, and fixed with paraformaldehyde (PFA) to achieve a final concentration of 0.5%. Samples were stained with SYBRTM-Green I nucleic acid gel stain (1:10,000 final dilution) and analyzed based on their PE-CF594 fluorescence and forward scatter (FSC) properties.

Before conducting the grazing experiment, we performed a preliminary study to determine the optimal algal concentrations. Five concentrations were tested: 500, 1000, 2000, 4000, and 6000 cells mL⁻¹ for *P. brasiliiana*, and 300, 600, 1200, 2400, and 3600 cells mL⁻¹ for *P. cuspidata*. Each concentration was added to experimental bottles (200 mL) containing 10 copepods, with control bottles containing no copepods. All experimental setups were replicated three times. The ingestion rate was calculated based on the method described by Yang et al. (2024) after determining the concentration at which ingestion was maximal. Ingestion rates were measured at the start (D0) and daily thereafter (D1-D5).

Respiration rates were measured using a SensorDish[®] reader (24-channel oxygen meter, PreSens, Germany) (Lelong et al. 2012). Copepods were washed with 0.2 μm filtered sterilized seawater and transferred to 2.5 mL sensor vials (PreSens, Germany). Each group contained six vials with copepods, and three other vials served as blank controls. These vials were filled with 0.2 μm -filtered sterilized seawater and placed in the SensorDish[®] reader to monitor O₂ concentration. O₂ concentration was recorded every 15 seconds for one hour. The respiration rate for each vial was determined by calculating the slope of the regression line of O₂ concentration versus time. The copepod respiration rate was obtained by subtracting the control vial readings from those of the vials containing copepods.

2.3 Gut dissection experiment of *A. erythraea* on different diets (Expt2.)

To obtain DNA and RNA from the gut microbiota of *A. erythraea*, gut dissections were performed on days 1 and 2 (D1 and D2) for both diets (Fig. 1). Guts were extracted using sterilized dissection tweezers (Regine 5, Switzerland) in a sterile Petri dish under a stereomicroscope (Stemi 305). The extracted guts were then transferred to 0.5 mL tubes containing 0.2 μm -filtered sterile seawater and kept on ice. Subsequently, the samples were filtered through a 0.2 μm polycarbonate membrane (IsoporeTM, 47 mm) and stored in 1 mL of Trizol Reagent (Sigma, USA). A total of 90 copepod guts were dissected per sample to ensure sufficient RNA yield. Three skilled experimenters conducted the dissections simultaneously, completing each sample within 30 minutes. These samples were designated for subsequent metatranscriptome analyses of gut microbiota and transcriptome analyses of copepod. Additionally, 12 guts were dissected from copepods on toxic and non-toxic, respectively, on D1 and D2, with each gut placed in separate 0.5 mL tubes for 16S V4 amplicon analysis. All samples were stored at -80°C for subsequent DNA and RNA extraction.

2.4 Gut microbiota community analysis

DNA extraction was performed using the DNeasy Blood & Tissue Kit (QIAGEN, Germany) according to the manufacturer's instructions. PCR amplification of bacterial 16S rRNA genes targeting the V4 region was conducted using primers 515F (5'-GTGCCAGCMGCCGCGGTAA-3'; Caporaso et al. 2011) and 806R (5'-GGACTACHVGGGTWTCTAAT-3'; Caporaso et al. 2011). The PCR reactions were set up in a 25 μL volume with Platinum Taq polymerase (Invitrogen, Waltham, MA, USA) and carried out in a Veriti 96-Well

Fast Thermal Cycler (Thermo Fisher Scientific, Waltham, MA, USA). The PCR protocol included an initial denaturation step at 94 for 3 minutes, followed by 35 cycles of denaturation at 94 for 45 seconds, annealing at 50 for 60 seconds, extension at 72 for 90 seconds, and a final extension at 72 for 10 minutes. PCRs were performed in triplicate, and the products were pooled and sequenced using the HiSeq 2500 System (Illumina, San Diego, CA, USA) with 2×250 bp paired-end read configurations.

The amplicon sequencing results were analyzed using the QIIME2 pipeline, adhering to established procedures for quality filtering, demultiplexing, and denoising with DADA2 (Callahan et al. 2016). Clustering into operational taxonomic units (OTUs) was performed at 97% similarity, followed by taxonomy assignment and diversity analysis. Taxonomic assignment of OTUs was conducted using the SILVA database (release 138). Prior to community structure analysis, OTU reads were normalized, and chloroplasts and mitochondria were removed. Additionally, OTUs with a relative abundance of less than 0.1% were filtered out. Paired t-tests and t-tests were performed using the R package “vegan” (Oksanen et al. 2007).

2.5 Gut microbiota metatranscriptome analysis

Total RNA extraction was conducted using the RNeasy Plus Mini Kit (QIAGEN, Germany) in accordance with the manufacturer’s protocol. The quality and integrity of the RNA were evaluated using a NanoDrop spectrophotometer (Thermo Fisher Scientific, MA, USA). Only samples that met the following criteria were utilized for further analysis: a 260/280 ratio between 1.8 and 2.1, and a 260/230 ratio between 2.0 and 2.4.

In total, we sequenced four transcriptome samples (one sample per group) and twelve metatranscriptome samples (triplicate samples per group). For eukaryotic RNA sequencing, one RNA sample from both toxic and non-toxic diets on D1 and D2 was processed using Poly(A) RNA sequencing (RNA-seq), selecting only RNAs with poly(A) tails, such as eukaryotic mRNAs. Library construction utilized poly-A oligo-attached magnetic beads. For both eukaryotic and prokaryotic RNA sequencing, triplicate RNA samples from the toxic and non-toxic diets on D1 and D2 were subjected to metatranscriptome sequencing, using all RNAs except ribosomal RNAs for library construction. RNA-seq and metatranscriptome sequencing were performed on a NovaSeq 6000 system (Illumina, CA, USA), generating 150-bp paired-end reads. Clean reads were obtained by removing adapters, barcodes, poly-N reads, and low-quality reads from the raw data. Quality control, assembly, and annotation of the transcriptome and metatranscriptome data were conducted following the methods described by Chen et al. (2024).

The host transcriptome was co-assembled using RNA-seq data with Trinity v2.14.0 (Grabherr et al. 2011). To obtain prokaryotic reads, the metatranscriptome reads were aligned to the host assembly, and the mapped reads were subsequently removed. Prokaryotic metatranscriptome reads were then co-assembled using Trinity v2.14.0 (Grabherr et al. 2011). Similar transcripts were clustered with CD-HIT (Fu et al. 2012) with ‘-c 0.95’ parameter, retaining a single representative transcript for each cluster. The longest open reading frame (ORF) for each transcript was identified using TransDecoder v5.5.0 (<https://github.com/TransDecoder/TransDecoder>) and annotated against the Kyoto Encyclopedia of Genes and Genomes (KEGG) (Kanehisa and Goto 2000) with ‘-sensitive -e 1e-20’ parameters.

Raw reads from the metatranscriptome were aligned to host assembly and prokaryotic assembly using Bowtie2 v2.4.4 (Langmead and Salzberg 2012) with default settings, respectively. Based on the results (SAM files) from Bowtie2, the read counts of all genes at all samples were summarized using featureCounts v.2.0.0 (Liao, Smyth, and Shi 2014) with the following parameters: ‘-M, -O, -fraction’. After separating the expressed gene profiles of the gut microbiota and *A. erythraea*, differentially expressed genes (DEGs) were identified using the edgeR v.3.30.3 R package (Robinson, McCarthy, and Smyth 2010). Genes with a P-value < 0.05 and $|\log_2(\text{fold change})| > 1$ were considered DEGs. KEGG enrichment analysis was performed using the ‘enricher’ function in the clusterProfiler v.3.16.1 R package (Yu et al. 2012), defining significantly enriched pathways as those with an adjusted p -value < 0.05 .

2.6 Cell death and proliferation staining of *A. erythraea*(Expt3.)

To further explore the effects of DA on copepods at the cellular level, we first cultured *A. erythraea* on

the two diets for 48h and then fixed them with 4% paraformaldehyde in phosphate-buffered saline (PBS). For the measurement of dead cells, the terminal deoxynucleotidyl transferase biotin-dUTP nick end labeling (TUNEL) assay was performed with an in situ cell death detection (TMR Red) kit according to the manufacturer’s instructions. Labelling and detection of proliferating cells in *A. erythraea* were performed using the Click-iT EdU Cell Proliferation Kit (Invitrogen), with the following modifications. *A. erythraea* were incubated in a 10 μ M solution of 5-Ethynyl-2-deoxyuridine (EdU) for 3 h immediately before fixation in a solution of 4% paraformaldehyde in PBS. The copepods were viewed and photographed with a Leica M205 FCA microscope equipped with a Leica DFC 7000T camera.

Results and Discussion

3.1 Gut microbes enhance the survival of *A. erythraea* on the DA diet

To investigate the DA resistance of *A. erythraea*, we fed the copepods toxic *P. cuspidata*, which had a DA concentration of 4.9 ± 0.7 fg cell⁻¹, as well as non-toxic *P. brasiliensis*. Our results indicate that the respiration rate of *A. erythraea* was significantly higher when fed the toxic diet compared to the non-toxic diet, starting from the second day ($p < 0.05$, t-test) (Fig. 2A). Ingestion rates peaked at 2000 cells mL⁻¹ (Fig. S1), which was used for subsequent daily measurements of *A. erythraea*’s ingestion rate on different *PSN* diets. In daily grazing experiments, *A. erythraea* maintained a consistent ingestion rate when fed the non-toxic *PSN*, averaging 2390 ± 359 cells copepod⁻¹ hour⁻¹. In contrast, the ingestion rate on the toxic diet showed a slight but significant decline starting from the second day ($p < 0.05$, t-test) (Fig. 2B). However, survival rates of *A. erythraea* over five days revealed no significant differences among the different diets (log-rank test, $p > 0.05$; Fig. 2A; Table S1). These results suggest that although the DA diets **suppressed** *A. erythraea* growth by reducing grazing and increasing respiration, it did not affect the survival of this copepod.

To further investigate the role of the gut microbiota of *A. erythraea* when copepods have a DA diet, we treated copepods on different diets with antibiotics and examined their survival. Before antibiotic treatment, each field-collected copepod **harbored** an average of 163,174 gut microbiota. After 24 hours of antibiotic treatment, the gut microbiota count per copepod decreased to 16,428, indicating an approximate 90% reduction (Figure S2). When *A. erythraea* was treated with antibiotics, resulting in a substantial reduction in gut microbiota, survival on the toxic diet was significantly lower than on the non-toxic diet (log-rank test, $p < 0.001$; Fig. 2A; Table S1). These findings suggest that the gut microbiota of *A. erythraea* plays a crucial role in detoxifying DA and enhancing survival on a DA diet.

3.2 Molecular responses of *A. erythraea* and its gut microbiota on a DA diet

To find the potential detoxification mechanisms associated with the DA diet, a metatranscriptome analysis was conducted. We analyzed the results of *A. erythraea* and gut microbiota separately. A total of 844 million raw reads were generated, resulting in 752 million clean reads. Among these, the average proportion of sequences mapped to *A. erythraea* was 26.69%, the average proportion mapped to gut microbiota was 8.62%, and the detailed proportions for each sample are provided in Table S2.

A. erythraea fed with toxic and non-toxic diets exhibited distinct gene expression profiles (Fig. S3A). Through KEGG enrichment analysis, we found that pathways involved in ingestion, such as protein digestion and absorption (map04974) and lysosome (map04142), were significantly **downregulated** on the toxic diet (Table S3). This finding is **consistent** with the **observed** reduction in grazing by *A. erythraea* on the toxic diet (Fig. 2A). **Additionally**, we found that processes **related to** cell death and cell proliferation were significantly **upregulated** on the toxic diet (Table S3), which was **further** supported by stronger TUNEL and EdU signals **observed in** the toxic diet (Fig. S4). **This suggests that** *A. erythraea* may accelerate cell proliferation to repair damaged cells and mitigate the adverse effects of DA.

We then examined the gene expression profiles of gut bacteria. Similar to copepods, the PCA plot revealed that the toxic and non-toxic diets clustered into distinct groups (Fig. 3A), indicating the different expression profiles between the two. Compared to the non-toxic group, *A. erythraea* exhibited 9,867 DEGs on the first

day (7,329 upregulated and 2,538 downregulated) and 23,871 DEGs on the second day (13,757 upregulated and 10,114 downregulated) (Fig. 3B). **To further investigate**, we conducted KEGG enrichment analysis on these DEGs to identify key pathways activated by DA diet. **In this context**, metabolism is the primary process involved in microbial detoxification and adaptation to toxicity. **Consequently**, we concentrated on the metabolic pathways that were significantly enriched (adjusted p -value < 0.05). Eight metabolic pathways were significantly upregulated on the first day, and twelve on the second day (Fig. 3C; Table S4).

3.3 The mechanisms of DA detoxification by the gut microbiota of *A. erythraea*

Microorganisms utilize multiple pathways for the biotransformation of DA (Du et al. 2022; Du et al. 2023; Li et al. 2024a; Li et al. 2024b). In our results, we observed a significant upregulation of the fatty acid degradation pathway (map00071) (Fig. 3C; Table S4). Specifically, as the main process of fatty acid degradation, fatty acid β -oxidation is also the crucial step in the DA biotransformation pathway (Fig. 4; Pathway 1) **proposed** by Du et al. (2022). Moreover, the involved genes such as *ACSL*, *fadI*, *fadJ*, and *fadN*, were all significantly upregulated in our findings ($p < 0.05$, Table S5). To achieve the anaerobic bioconversion of DA to the non-toxic compound P215-type I (Fig. 4; Pathway 1), additional steps are necessary beyond β -oxidation, including decarboxylation, dehydrogenation, and carboxylation (Du et al. 2022). Key genes involved in these processes, such as *panD*, *adhP*, and *pyc*, were also significantly upregulated ($p < 0.05$, Table S5). To obtain these upregulated DEGs taxonomic information, we conducted a BLAST search of the nucleotide sequences of these DEGs against the Nr database (Table S5). In this pathway, *Neobacillus sp.* upregulated the *panD* gene, which encodes aspartate 1-decarboxylase and catalyzes the first decarboxylation reaction in this pathway. In the subsequent step, *Aureispira sp.* significantly upregulated the *pyc* gene, which encodes pyruvate carboxylase and facilitates the carboxylation of P281. This species is also involved in the β -oxidation step of P325, upregulating the *ACSL*, *fadI*, *fadJ*, and *fadN* genes, which promote the transformation of P325 to P215-type I. Additionally, *Tenacibaculum sp.*, *Pseudoalteromonas sp.*, *Shewanella sp.*, and *Vibrio sp.* also participate in the β -oxidation step of this pathway (Fig. 4).

In addition, Li et al. (2024a) proposed that microbial amino acid metabolism drives the degradation of DA in sediments and suggested another DA biotransformation pathway (Pathway 2). Our results indicated that amino acid metabolism pathways, including alanine, aspartate, and glutamate metabolism (map00250), cysteine and methionine metabolism (map00270), and valine, leucine, and isoleucine degradation (map00280), were all significantly induced on the second day. We predict that more DA will be taken up or accumulated on the second day compared to the first, and these processes are dose-dependent. Among these pathways, the genes *gadA*, *fadJ*, and *fadI*, which are involved in amino acid metabolism, were significantly upregulated ($p < 0.05$) and also play a role in DA biotransformation. Furthermore, the genes *mgo*, *putB*, and *ACSL* were significantly upregulated ($p < 0.05$), contributing importantly to this DA biotransformation pathway. Ultimately, DA is converted into P215-type II, a long-chain unsaturated fatty acid, which is subsequently cleaved into short-chain fatty acids in the TCA cycle and ultimately mineralized (Li et al. 2024a). In this pathway, along with the β -oxidation steps involving the genes *ACSL*, *fadJ*, and *fadI*, *Alteromonas sp.* upregulated the *gadA* gene, which encodes glutamate decarboxylase and facilitates the decarboxylation of the intermediate product P273.

Lastly, Li et al. (2024b) also described the mechanism of aerobic DA degradation in *Pseudoalteromonas sp.* (Pathway 3), identifying *ldh*, *nqrA*, and *nqrF* as key genes, which are responsible for **hydroxylation**, decarboxylation and oxidation of DA and its intermediates. Our results demonstrated a significant upregulation of *nqrA* and *nqrF* ($p < 0.05$). In this pathway, *Pseudoalteromonas sp.*, *Aureispira sp.*, *Vibrio sp.*, *Tenacibaculum sp.*, and other unidentified bacteria upregulated the *nqrA* and *nqrF* genes, which encode the Na^+ -translocating NADH-quinone oxidoreductase. The enzyme catalyzes the production of biogenic O_2^- , facilitating the conversion of the intermediate P301 to P215-type I.

Notably, rather than a single bacterial group, multiple microorganisms are involved in all three DA biotransformation pathways. Similarly, Li et al. (2024a) pointed out that during the DA degradation process in sediments, the microbial community transitioned from nutritional competition to metabolic interrelationships, with DA enhancing cooperation among microbiota. We compared the relative abundance of these

taxa at the genus level based on 16S rRNA analysis. Taxa such as *Aureispira sp.*, *Pseudoalteromonas sp.*, *Tenacibaculum sp.*, *Vibrio sp.*, and *Shewanella sp.* exhibited higher abundance on the DA diet (Fig. 5). This increased relative abundance suggests that these bacteria have a competitive advantage on the toxic diet, potentially due to their ability to biotransform DA. Previous studies have reported that *Pseudoalteromonas sp.* possesses the capability to degrade DA (Li et al. 2024b). Additionally, Coral and Yildirim (2014) found that concentrations of 2.5 $\mu\text{g/ml}$ and 5 $\mu\text{g/ml}$ of DA induce growth in certain marine *Vibrio* strains isolated from Iskenderun Bay and Samandag shore.

These five genera also play significant roles in various steps of both aerobic and anaerobic DA biotransformation (Fig. 4). Our results strongly suggest that *Aureispira sp.*, *Tenacibaculum sp.*, *Pseudoalteromonas sp.*, *Shewanella sp.*, and *Vibrio sp.* are potential detoxifying gut microbiota that interact with one another to assist *A. erythraea* in detoxifying DA. This conclusion is supported by their higher relative abundance in the toxic diet and by their upregulation of detoxification-related genes.

Besides, we also noted that the drug metabolism - other enzymes pathway (map00983) was significantly upregulated as a component of the detoxification process. Within this pathway, three DEGs encoding glutathione S-transferase (GST) were significantly upregulated. GSTs are crucial enzymes involved in phase II detoxification of various xenobiotics, catalyzing the conjugation of reduced glutathione (GSH) to the electrophilic centers of xenobiotics, thereby probably facilitating detoxification (Li, Schuler, and Berenbaum 2007). This process may also contribute to DA detoxification.

During the detoxification of DA, several metabolic processes that contribute to energy production were significantly enhanced, including the TCA cycle (map00020), oxidative phosphorylation (map00190), glycolysis/gluconeogenesis (map00010), and the metabolism of certain amino acids and fatty acid β -oxidation (Fig. 3C). Key rate-limiting enzymes of the TCA cycle, such as citrate synthase (K01647), isocitrate dehydrogenase (K00030 and K00031), and the E1 (K00164) and E2 (K00658) components of 2-oxoglutarate dehydrogenase, were significantly upregulated ($p < 0.05$, Table S6). The TCA cycle generates NADH, which drives ATP production in the oxidative phosphorylation pathway (Oexle, Gnaiger, and Weiss 1999). Fatty acid β -oxidation is a crucial metabolic pathway for maintaining energy homeostasis when glucose supply is limited (Houten and Wanders 2010), and it also provides acetyl-CoA to the TCA cycle. Additionally, amino acid catabolism can contribute to energy production, with precursors such as pyruvate and other intermediates (e.g., acetyl-CoA, succinyl-CoA, and succinate from the TCA cycle) being replenished through amino acid metabolism. These results suggest that under the DA diet, microbial energy input is elevated, likely to meet the demands of DA detoxification or other defensive mechanisms.

Conclusion

This study employed a combined physiological and multi-omics approach, including amplicon and metatranscriptomic analyses, to explore how gut microbiota assist copepods in detoxifying DA diet. Our findings indicate that, although DA diet suppressed the growth of *A. erythraea*, the gut microbiota of *A. erythraea* plays a crucial role in detoxifying DA, thereby enhancing their survival on a toxic diet. We observed that the gut microbiota of *A. erythraea* upregulated several DA biotransformation genes, including *ACSL*, *fadI*, *fadJ*, *fadN*, *panD*, *adhP*, *pyc*, *gadA*, *mgo*, *putB*, *nqrA*, and *nqrF*, when DA producing PSN was ingested. This upregulation facilitates three biotransformations of DA, encompassing both anaerobic and aerobic transformations, ultimately aiding the host copepod in overcoming the toxic effects of DA. Additionally, we identified five taxa, i.e., *Aureispira sp.*, *Tenacibaculum sp.*, *Pseudoalteromonas sp.*, *Shewanella sp.*, and *Vibrio sp.*, as potential detoxification taxa. These taxa not only exhibited higher relative abundance in the toxic diet but also showed increased expression of DA biotransformation genes.

Author contribution

Qihang Li: conceptualization, investigation, methodology, software, visualization, writing-original draft, writing-review and editing. Jiawei Chen: conceptualization, data analysis, software, supervision, writing-

review and editing. Zhimeng Xu: investigation, methodology, data analysis. Lixia Deng: software, writing-review & editing. Xihe Fang: investigation. Shuwen Zhang: resources. Xiaodong Zhang: resources. Huo Xu: resources. Shen Lin: methodology, resources. Hongbin Liu: conceptualization, funding acquisition, resources, supervision, writing-review and editing.

Acknowledgements

We thank Dr. Niu Biaobiao of South China Normal University for his help in *PSN* isolation and culture. This work was supported by the Hong Kong Research Grants Council (16101622) and the Area of Excellence Scheme (AoE/P-601/23-N).

Conflicts of Interest

The authors declare no conflicts of interest.

Data Availability

The amplicon data have been deposited at the National Center for Biotechnology Information (NCBI) under BioProject PRJNAxxxx. Metatranscriptome data have been deposited at the National Center for Biotechnology Information (NCBI) under BioProject PRJNAxxxx, transcriptome data under BioProject PRJNAxxxx.

References

- Bates, Stephen S, David L Garrison, and Rita A Horner. 1998. 'Bloom dynamics and physiology of domoic acid-producing *Pseudo-nitzschia* species', *NATO ASI series G ecological sciences* , 41: 267-92.
- Bates, Stephen S, Katherine A Hubbard, Nina Lundholm, Marina Montresor, and Chui Pin Leaw. 2018. '*Pseudo-nitzschia* , *Nitzschia* , and domoic acid: New research since 2011', *Harmful Algae* , 79: 3-43.
- Callahan, Benjamin J, Paul J McMurdie, Michael J Rosen, Andrew W Han, Amy Jo A Johnson, and Susan P Holmes. 2016. 'DADA2: High-resolution sample inference from Illumina amplicon data', *Nature Methods* , 13: 581-83.
- Caporaso, J Gregory, Christian L Lauber, William A Walters, Donna Berg-Lyons, Catherine A Lozupone, Peter J Turnbaugh, Noah Fierer, and Rob Knight. 2011. 'Global patterns of 16S rRNA diversity at a depth of millions of sequences per sample', *Proceedings of the National Academy of Sciences* , 108: 4516-22.
- Carvalho Pinto-Silva, CR, S Moukha, WG Matias, and EE Creppy. 2008. 'Domoic acid induces direct DNA damage and apoptosis in Caco-2 cells: Recent advances', *Environmental Toxicology: An International Journal* , 23: 657-63.
- Chen, Jiawei, Lixia Deng, Mengwen Pang, Yingdong Li, Zhimeng Xu, Xiaodong Zhang, and Hongbin Liu. 2024. 'Transcriptomic insights into the shift of trophic strategies in mixotrophic dinoflagellate *Lepidodinium* in the warming ocean', *ISME Communications* : ycae087.
- Chen, Ju-fang, Yu-zao Qi, Xu,ning, Tian-jiu Jing, and Songhui LÜ. 2005. '*Pseudo-nitzschia* bloom and its ecological role in the biological community in the Daya Bay, the South China Sea', *Acta Oceanologica Sinica* , 27: 114-19.
- Coral, M Nisa Unaldi, and Aydil Yildirim. 2014. 'Effect of domoic acid on growth and heavy metal tolerance of some marine bacteria isolated from Samandag shore and Iskenderun bay', *Journal of Pure and Applied Microbiology* , 8: 1597-602.
- D'Agostino, Valeria C, Mariana Degradi, Viviana Sastre, Norma Santinelli, Bernd Krock, Torben Krohn, Silvana L Dans, and Mónica S Hoffmeyer. 2017. 'Domoic acid in a marine pelagic food web: Exposure of southern right whales *Eubalaena australis* to domoic acid on the Península Valdés calving ground, Argentina', *Harmful Algae* , 68: 248-57.
- Dong, Huan Chang, Nina Lundholm, Sing Tung Teng, Aifeng Li, Chao Wang, Yang Hu, and Yang Li. 2020. 'Occurrence of *Pseudo-nitzschia* species and associated domoic acid production along the Guangdong coast, South China Sea', *Harmful Algae* , 98: 101899.
- Du, Miaomiao, Yuan Jin, Jingfeng Fan, Shuaijun Zan, Chen Gu, and Jing Wang. 2023. 'A new pathway for anaerobic biotransformation of marine toxin domoic acid', *Environmental Science and Pollution Research* , 30: 5150-60.
- Du, Miaomiao, Zelong Li, Jing Wang, Fengbo Wang, Shuaijun Zan, and Chen Gu. 2022. 'Anaerobic biotransformation mechanism of marine toxin domoic acid', *Journal of Hazardous Materials* , 421: 126798.
- Edlund, Anna, Karin Ek, Magnus Breitholtz, and Elena Gorokhova. 2012. 'Antibiotic-induced change of bacterial communities associated with the copepod *Nitocra spinipes*', *PLoS One* , 7: e33107.
- Fu, Limin, Beifang Niu, Zhengwei Zhu, Sitao Wu, and Weizhong Li. 2012. 'CD-HIT: accelerated for clustering the next-generation sequencing data', *Bioinformatics* , 28: 3150-52.
- Gorokhova, Elena, Rehab El-Shehawey, Maiju Lehtiniemi, and Andrius Garbaras. 2021. 'How copepods

can eat toxins without getting sick: Gut bacteria help zooplankton to feed in cyanobacteria blooms', *Frontiers in Microbiology* , 11: 589816.Grabherr, Manfred G, Brian J Haas, Moran Yassour, Joshua Z Levin, Dawn A Thompson, Ido Amit, Xian Adiconis, Lin Fan, Raktima Raychowdhury, and Qiandong Zeng. 2011. 'Trinity: reconstructing a full-length transcriptome without a genome from RNA-Seq data', *Nature biotechnology* , 29: 644.Guillard, Robert RL, and John H Ryther. 1962. 'Studies of marine planktonic diatoms: I. *Cyclotella nana* Hustedt, and *Detonula confervacea* (Cleve) Gran', *Canadian Journal of Microbiology* , 8: 229-39.Harardóttir, Sara, Ditte Marie Hjort, Sylke Wohlrab, Bernd Krock, Uwe John, Torkel Gissel Nielsen, and Nina Lundholm. 2019. 'Trophic interactions, toxicokinetics, and detoxification processes in a domoic acid-producing diatom and two copepod species', *Limnology and Oceanography* , 64: 833-48.Hardardottir, Sara, Bernd Krock, Sylke Wohlrab, Uwe John, Torkel Gissel Nielsen, and Nina Lundholm. 2018. 'Can domoic acid affect escape response in copepods?', *Harmful Algae* , 79: 50-52.Harris, Jean M. 1993. 'The presence, nature, and role of gut microflora in aquatic invertebrates: a synthesis', *Microbial Ecology* , 25: 195-231.Houten, Sander Michel, and Ronald JA Wanders. 2010. 'A general introduction to the biochemistry of mitochondrial fatty acid β -oxidation', *Journal of Inherited Metabolic Disease* , 33: 469-77.Huang, Chun Xiu, Huan Chang Dong, Nina Lundholm, Sing Tung Teng, Guan Chao Zheng, Zhi Jun Tan, Po Teen Lim, and Yang Li. 2019. 'Species composition and toxicity of the genus *Pseudo-nitzschia* in Taiwan Strait, including *P. chiniana* sp. nov. and *P. qiana* sp. nov', *Harmful Algae* , 84: 195-209.Kanehisa, Minoru, and Susumu Goto. 2000. 'KEGG: kyoto encyclopedia of genes and genomes', *Nucleic Acids Research* , 28: 27-30.Langmead, Ben, and Steven L Salzberg. 2012. 'Fast gapped-read alignment with Bowtie 2', *Nature Methods* , 9: 357-59.Leandro, Luis F, Gregory J Teegarden, Patricia B Roth, Zhihong Wang, and Gregory J Doucette. 2010. 'The copepod *Calanus finmarchicus* : A potential vector for trophic transfer of the marine algal biotoxin, domoic acid', *Journal of Experimental Marine Biology and Ecology* , 382: 88-95.Lelong, Aurélie, Dianne F Jolley, Philippe Soudant, and Hélène Hégaret. 2012. 'Impact of copper exposure on *Pseudo-nitzschia* spp. physiology and domoic acid production', *Aquatic Toxicology* , 118: 37-47.Li, Xianchun, Mary A Schuler, and May R Berenbaum. 2007. 'Molecular mechanisms of metabolic resistance to synthetic and natural xenobiotics', *Annual Review of Entomology* , 52: 231-53.Li, Yang, Chun Xiu Huang, Guo Shuang Xu, Nina Lundholm, Sing Tung Teng, Haiyan Wu, and Zhijun Tan. 2017. '*Pseudo-nitzschia simulans* sp. nov.(Bacillariophyceae), the first domoic acid producer from Chinese waters', *Harmful Algae* , 67: 119-30.Li, Yingdong, Wen-Xiong Wang, and Hongbin Liu. 2022. 'Gut-microbial adaptation and transformation of silver nanoparticles mediated the detoxification of *Daphnia magna* and their offspring', *Environmental Science: Nano* , 9: 361-74.Li, Yingdong, Neng Yan, Tin Yan Wong, Wen-Xiong Wang, and Hongbin Liu. 2019. 'Interaction of antibacterial silver nanoparticles and microbiota-dependent holobionts revealed by metatranscriptomic analysis', *Environmental Science: Nano* , 6: 3242-55.Li, Zelong, Jing Wang, Mariam Yousaf, Arbaz Rehman, and Fengbo Wang. 2024b. 'Biogenic ROS mediated degradation mechanism of marine toxin domoic acid', *Science of The Total Environment* , 953: 176039.Li, Zelong, Jing Wang, Hao Yue, Miaomiao Du, Yuan Jin, and Jingfeng Fan. 2023. 'Marine toxin domoic acid alters nitrogen cycling in sediments', *Nature Communications* , 14: 7873.Li, Zelong, Jing Wang, Hao Yue, Arbaz Rehman, Mariam Yousaf, Miaomiao Du, and Xiuhong Zhang. 2024a. 'Applying metabolic modeling and multi-omics to elucidate the biotransformation mechanisms of marine algal toxin domoic acid (DA) in sediments', *Journal of Hazardous Materials* , 472: 134541.Liao, Yang, Gordon K Smyth, and Wei Shi. 2014. 'featureCounts: an efficient general purpose program for assigning sequence reads to genomic features', *Bioinformatics* , 30: 923-30.Liefer, Justin D, Alison Robertson, Hugh L MacIntyre, William L Smith, and Carol P Dorsey. 2013. 'Characterization of a toxic *Pseudo-nitzschia* spp. bloom in the Northern Gulf of Mexico associated with domoic acid accumulation in fish', *Harmful Algae* , 26: 20-32.Lincoln, Jean A, Jefferson T Turner, Stephen S Bates, Claude Léger, and David A Gauthier. 2001. 'Feeding, egg production, and egg hatching success of the copepods *Acartia tonsa* and *Temora longicornis* on diets of the toxic diatom *Pseudo-nitzschia multiseriata* and the non-toxic diatom *Pseudo-nitzschia pungens* ', *Hydrobiologia* , 453: 107-20.Liu, RY, L Liu, YB Liang, J Yu, DY Xu, N Wei, L Yang, and H Guo. 2016. 'The distribution, impacts and risks of toxic microalgae and phycotoxins in China', *Marine Environmental Science* , 35: 787-800.Loo, Deryk T. 2011. 'In situ detection of apoptosis by the TUNEL assay: an overview of techniques', *DNA Damage Detection In Situ, Ex Vivo, and In Vivo: Methods and Protocols* : 3-13.Lü, Songhui, Yang Li, Nina Lundholm, Yanyan Ma, and KC Ho. 2012. 'Diversity, taxonomy and biogeographical distribution of the genus

Pseudo-nitzschia (Bacillariophyceae) in Guangdong coastal waters, South China Sea', *Nova Hedwigia* , 95: 123. Lundholm, N.; Churro, C.; Escalera, L.; Fraga, S.; Hoppenrath, M.; Iwataki, M.; Larsen, J.; Mertens, K.; Moestrup, Ø.; Murray, S.; Tillmann, U.; Zingone, A. 2024. "IOC-UNESCO Taxonomic Reference List of Harmful Micro Algae." In. <https://www.marinespecies.org/hab>.

Lyu, Kai, Haoyong Guan, Changcan Wu, Xingyu Wang, Alan E Wilson, and Zhou Yang. 2016. 'Maternal consumption of non-toxic *Microcystis* by *Daphnia magna* induces tolerance to toxic *Microcystis* in offspring', *Freshwater Biology* , 61: 219-28.

Macke, Emilie, Martijn Callens, Luc De Meester, and Ellen Decaestecker. 2017. 'Host-genotype dependent gut microbiota drives zooplankton tolerance to toxic cyanobacteria', *Nature Communications* , 8: 1608.

Maneiro, Isabel, Paula Iglesias, Castor Guisande, Isabel Riveiro, Aldo Barreiro, Sultana Zervoudaki, and Edna Graneli. 2005. 'Fate of domoic acid ingested by the copepod *Acartia clausi* ', *Marine Biology* , 148: 123-30.

Miesner, Anna K, Nina Lundholm, Bernd Krock, and Torkel Gissel Nielsen. 2016. 'The effect of *Pseudo-nitzschia* seriata on grazing and fecundity of *Calanus finmarchicus* and *Calanus glacialis* ', *Journal of Plankton Research* , 38: 564-74.

Niu, Biao-Biao, Qi-Xiang Zheng, Yang Liu, Nina Lundholm, Sing Tung Teng, Xu-Dan Lu, Rui-Wei Ran, Li Zhang, and Yang Li. 2024. 'Morphology, molecular phylogeny and biogeography revealed two new *Pseudo-nitzschia* (Bacillariophyceae) species in Chinese waters', *Journal of Systematics and Evolution* , 62: 621-36.

Oexle, Horst, Erich Gnaiger, and Gunter Weiss. 1999. 'Iron-dependent changes in cellular energy metabolism: influence on citric acid cycle and oxidative phosphorylation', *Biochimica et Biophysica Acta (BBA)-Bioenergetics* , 1413: 99-107.

Oksanen, J, R Kindt, P Legendre, B O'hara, MHH Stevens, MJ Oksanen, and MASS Suggests. 2007. 'The vegan package: community ecology package', *R package version* , 1: 1-190.

Robinson, Mark D, Davis J McCarthy, and Gordon K Smyth. 2010. 'edgeR: a Bioconductor package for differential expression analysis of digital gene expression data', *Bioinformatics* , 26: 139-40.

Shoemaker, Katyanne M, and Pia H Moisaner. 2017. 'Seasonal variation in the copepod gut microbiome in the subtropical North Atlantic Ocean', *Environmental Microbiology* , 19: 3087-97.

Tammilehto, Anna, Torkel Gissel Nielsen, Bernd Krock, Eva Friis Moller, and Nina Lundholm. 2012. '*Calanus* spp. — Vectors for the biotoxin, domoic acid, in the Arctic marine ecosystem?', *Harmful Algae* , 20: 165-74.

Tester, Patricia A, Youlian Pan, Gregory J Doucette, and CA Scholin. 2000. 'Accumulation of domoic acid activity in copepods', *Harmful Algal Blooms* : 418-21.

Wright, JL, CJ Bird, AS De Freitas, D Hampson, J McDonald, and MA Quilliam. 1990. 'Chemistry, biology, and toxicology of domoic acid and its isomers', *Canada Diseases Weekly Report= Rapport Hebdomadaire des Maladies au Canada* , 16: 21-26.

Yang, Jing, Zhimeng Xu, Yi Chen, Huo Xu, Zuyuan Gao, Xiaodong Zhang, Mengwen Pang, Shuwen Zhang, and Hongbin Liu. 2024. 'Community changes of gut microbes highlight their importance in the adaptation of copepods to toxic dinoflagellates', *Frontiers in Marine Science* , 11: 1368315.

Yu, Guangchuang, Li-Gen Wang, Yanyan Han, and Qing-Yu He. 2012. 'clusterProfiler: an R package for comparing biological themes among gene clusters', *Omics: a Journal of Integrative Biology* , 16: 284-87.

Figure

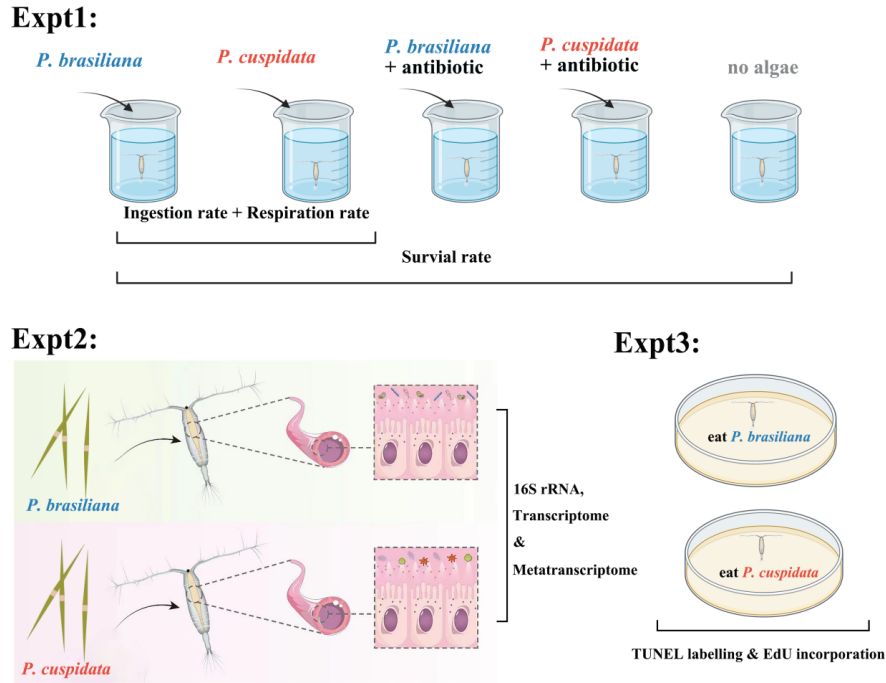


Figure 1 | Schematic diagram showing the experimental procedure. Experiment 1 (Expt1): Antibiotic experiment and physiological monitoring of *A. erythraea*; Experiment 2 (Expt2): Gut dissection and omics analysis of *A. erythraea* on different diets; Experiment 3 (Expt3): Cell death and proliferation staining of *A. erythraea*. Cell death was labelled by terminal deoxynucleotidyl transferase biotin-dUTP nick end labelling (TUNEL), and cell proliferation was measured by 5-Ethynyl-2-deoxyuridine (EdU) incorporation.

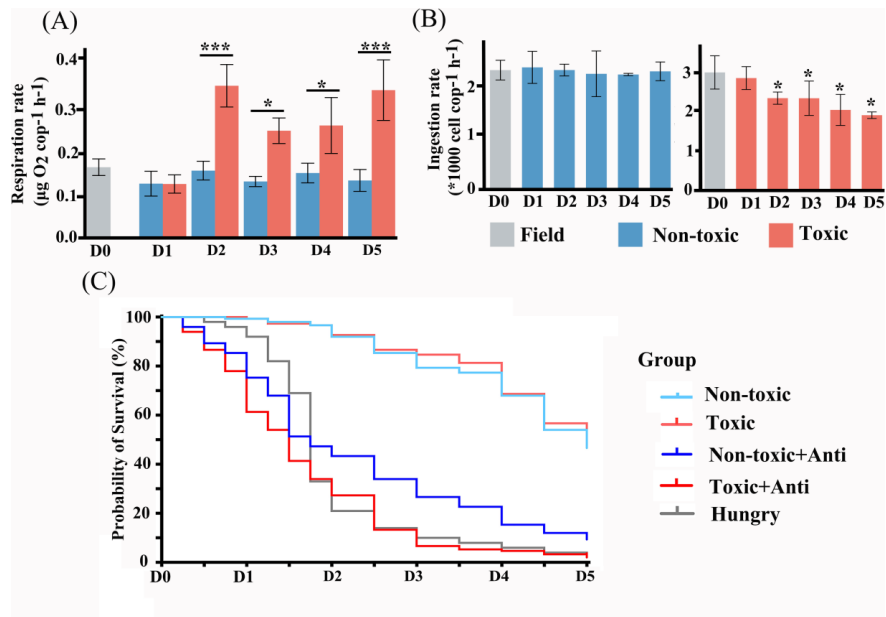


Figure 2 | Physiological changes of *A. erythraea* over time under different diets and treatments. (A) Respiration rate. The significance test for respiration rate was a t-test between the toxic group and the

non-toxic group on the same day. (B) Ingestion rate. The field group represents copepods that have not been cultured in the laboratory. The significance test for ingestion rate is a t-test comparing the toxic/non-toxic group with the field group. ($*p < 0.05$; $**p < 0.01$; $***p < 0.001$). (C) The non-toxic and toxic groups represent copepods fed exclusively with *P. brasiliensis* and *P. cuspidata*, respectively. The Non-toxic+Anti and Toxic+Anti groups received the same algal diet with the addition of antibiotics. The hungry group consists of copepods that were not provided with an algal supply.

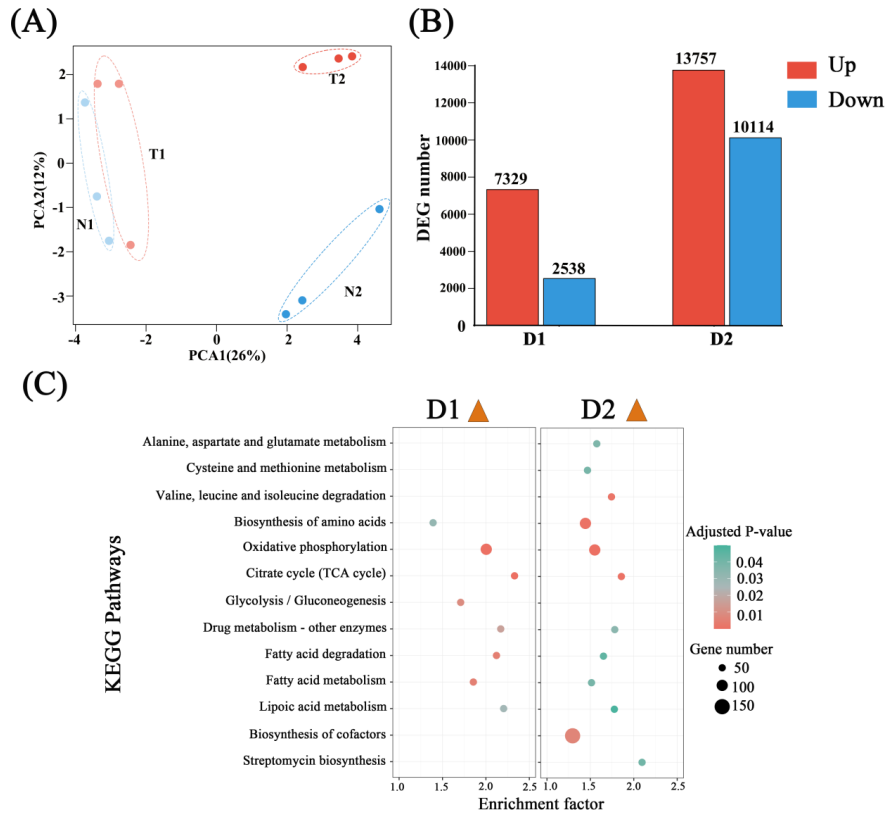


Figure 3 | Overview of gene expression profiles by gut microbiota. (A) Principal component analysis (PCA) of different treatment. N1 represents the first day (D1) of the non-toxic diet, N2 represents the second day (D2) of the non-toxic diet, T1 represents D1 of the toxic diet, T2 represents D2 of the toxic diet. (B) Differentially expressed gene (DEG) number; (C) Significantly enriched and upregulated metabolic pathways.

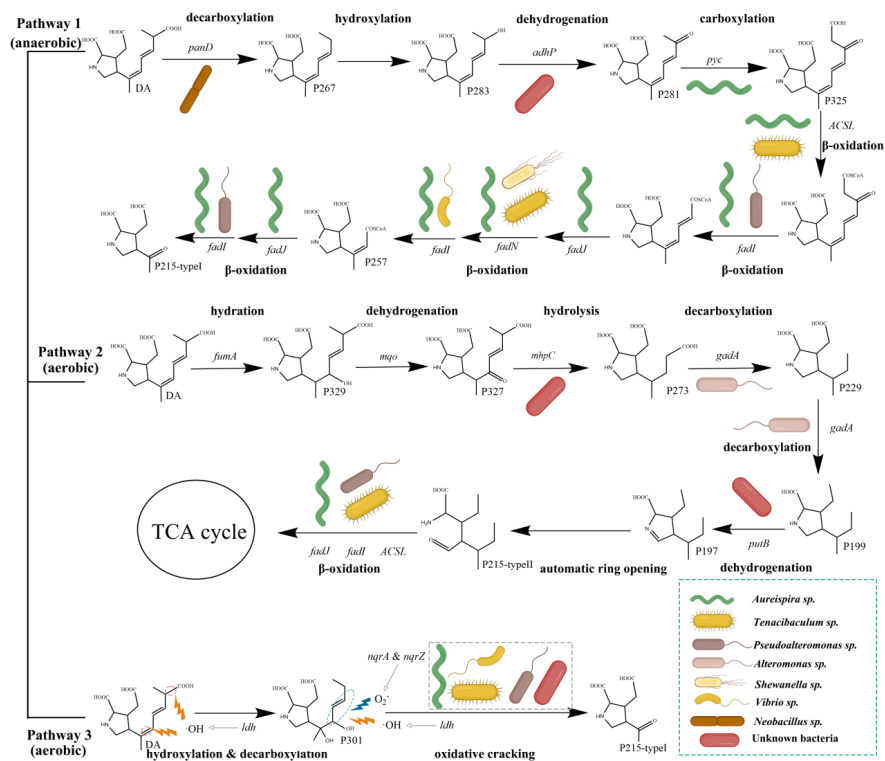


Figure 4 | Composition of gut microbiota involved in each step of DA biotransformation.

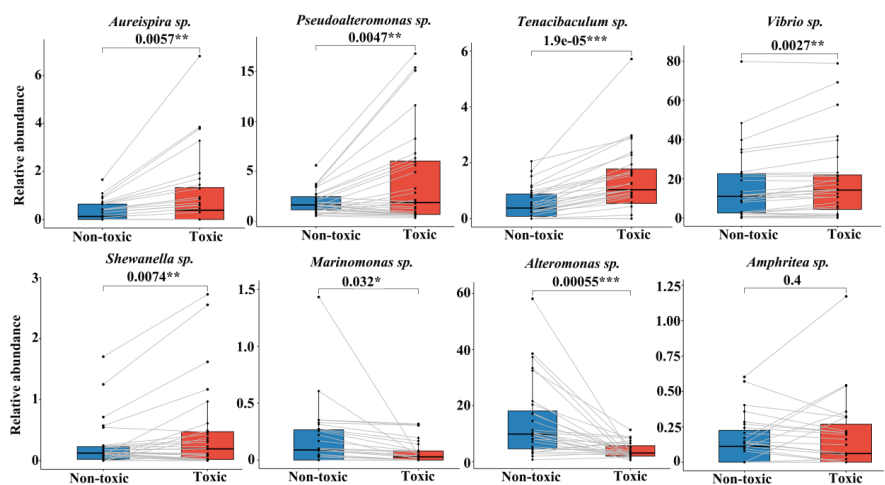


Figure 5 | Comparison of relative abundance of gut microbiota under different diets